ARTICLES
PUBLISHED ONLINE: 14 JULY 2013 | DOI: 10.1038/NNANO.2013.132
nature nanotechnology

Molecular crowding shapes gene expression in synthetic cellular nanosystems

Cheemeng Tan[1], Saumya Saurabh[2,3], Marcel P. Bruchez[2,3,4], Russell Schwartz[1,4]* and Philip LeDuc[1,4,5]*

The integration of synthetic and cell-free biology has made tremendous strides towards creating artificial cellular nanosystems using concepts from solution-based chemistry, where only the concentrations of reacting species modulate gene expression rates. However, it is known that macromolecular crowding, a key feature in natural cells, can dramatically influence biochemical kinetics via volume exclusion effects, which reduce diffusion rates and enhance binding rates of macromolecules. Here, we demonstrate that macromolecular crowding can increase the robustness of gene expression by integrating synthetic cellular components of biological circuits and artificial cellular nanosystems. Furthermore, we reveal how ubiquitous cellular modules, including genetic components, a negative feedback loop and the size of the crowding molecules can fine-tune gene circuit response to molecular crowding. By bridging a key gap between artificial and living cells, our work has implications for efficient and robust control of both synthetic and natural cellular circuits.

An overarching desire to harness natural biological principles for biotechnological applications has driven synthetic biology towards the creation of cells with completely synthetic genomes[1] or genetic polymers[2], synthetic organisms with hybrid cellular and polymeric structures[3], synthetic *in vitro* systems[4] and artificial cells with synthetic components[5–12]. These synthetic and hybrid systems have tremendous potential for novel applications in the discovery of fundamental biological principles[13], therapeutic treatment[14] and bioenergy production[15], as they enable more precise control and predictive modelling of systems by minimizing cellular components. However, although reducing the complexity of the systems allows more precise control of the reaction environment, it also has the potential to eliminate features of the cellular micro-environment that are important for the robust functioning of genetic circuits. One key distinguishing feature between living cells and the prevailing artificial cellular systems is the density of molecules around cellular components, which is an under-appreciated, yet important factor in the regulation of cellular dynamics[16,17].

Molecular crowding is a natural state of cells in which their intracellular environments are densely packed with macromolecules[18,19] (Fig. 1a). This crowding is absent in the solution-based chemistry approaches that are typically used in synthetic genetic systems. Molecular crowding can cause volume exclusion effects that reduce diffusion rates and enhance the binding rates of macromolecules[20], leading to a fundamental impact on cellular properties such as the optimum number of transcription factors[21], the dynamical order of metabolic pathways[22] and nuclear architecture[23]. However, the impacts of molecular crowding on the dynamics of gene circuits and the consequences for their activity in heterologous environments have not been established. It remains unclear whether molecular crowding can increase the robustness of gene expression towards perturbations of genetic micro-environments. Furthermore, there have been tremendous controversies regarding whether molecular crowding can indeed impact cellular activities[24–26]. Answers to these fundamental questions would enable more precise control of synthetic gene circuits in artificial systems, provide a bridge between *in vitro* and *in vivo* systems[24], and facilitate predictive approaches for both synthetic and natural biological systems.

Impact on diffusion of T7 RNA polymerase

To investigate the impact of molecular crowding on gene expression, we used genetic components from phage T7 because of their well-characterized kinetics and functions in synthetic systems (Supplementary Fig. S1). We quantified interactions between T7 RNA polymerase (RNAP) and DNA in the presence of crowding agents because molecular crowding can increase excluded volumes, which will affect large molecules to a greater extent than small molecules[19]. To visualize the response, we constructed a red fluorescent protein (RFP)–T7 RNAP fusion RNA polymerase that transcribes a cyan fluorescent protein (CFP) from a P_{T7} promoter (Supplementary Fig. S2a, b and Supplementary section 'Cloning of pTet-TagRFP-T7RNAP').

Because transcriptional activities are sensitive to the diffusion of macromolecules[21], we first focused on the diffusion dynamics of T7 RNAP in different crowding environments outside the artificial cell environment. We modulated the crowding molecule size, because a previous work has suggested that natural cells could use crowding molecules as molecular sieves to filter molecules and modulate system dynamics[27]. Specifically, we performed fluorescence recovery after photobleaching (FRAP, Supplementary Fig. S3, Movie S1) using small (6×10^3 g mol^{-1}, Dex-Small) or big (2×10^6 g mol^{-1}, Dex-Big) dextran polymers (Fig. 1b,c). These molecules are commonly used as inert molecules to mimic crowded intracellular environments, and do not react with the systems of interest[28]. We found that the initial recovery rates of mobile RFP–T7 RNAP were significantly reduced on increasing the densities of both Dex-Small and Dex-Big molecules (Fig. 1b, Supplementary Fig. S3b). This result suggests that diffusion of the mobile fraction of RFP–T7 RNAP is affected by the crowding molecules. Increasing the crowding densities using both Dex-Small and Dex-Big also resulted in higher immobile fractions of RFP–T7

[1]Lane Center for Computational Biology, Carnegie Mellon University, Pittsburgh, Pennsylvania 15213, USA, [2]Department of Chemistry, Carnegie Mellon University, Pittsburgh, Pennsylvania 15213, USA, [3]Molecular Biosensor and Imaging Center, Carnegie Mellon University, Pittsburgh, Pennsylvania 15213, USA, [4]Department of Biological Sciences, Carnegie Mellon University, Pittsburgh, Pennsylvania 15213, USA, [5]Department of Mechanical Engineering and Biomedical Engineering, Carnegie Mellon University, Pittsburgh, Pennsylvania 15213, USA. *e-mail: prl@andrew.cmu.edu; russell@andrew.cmu.edu

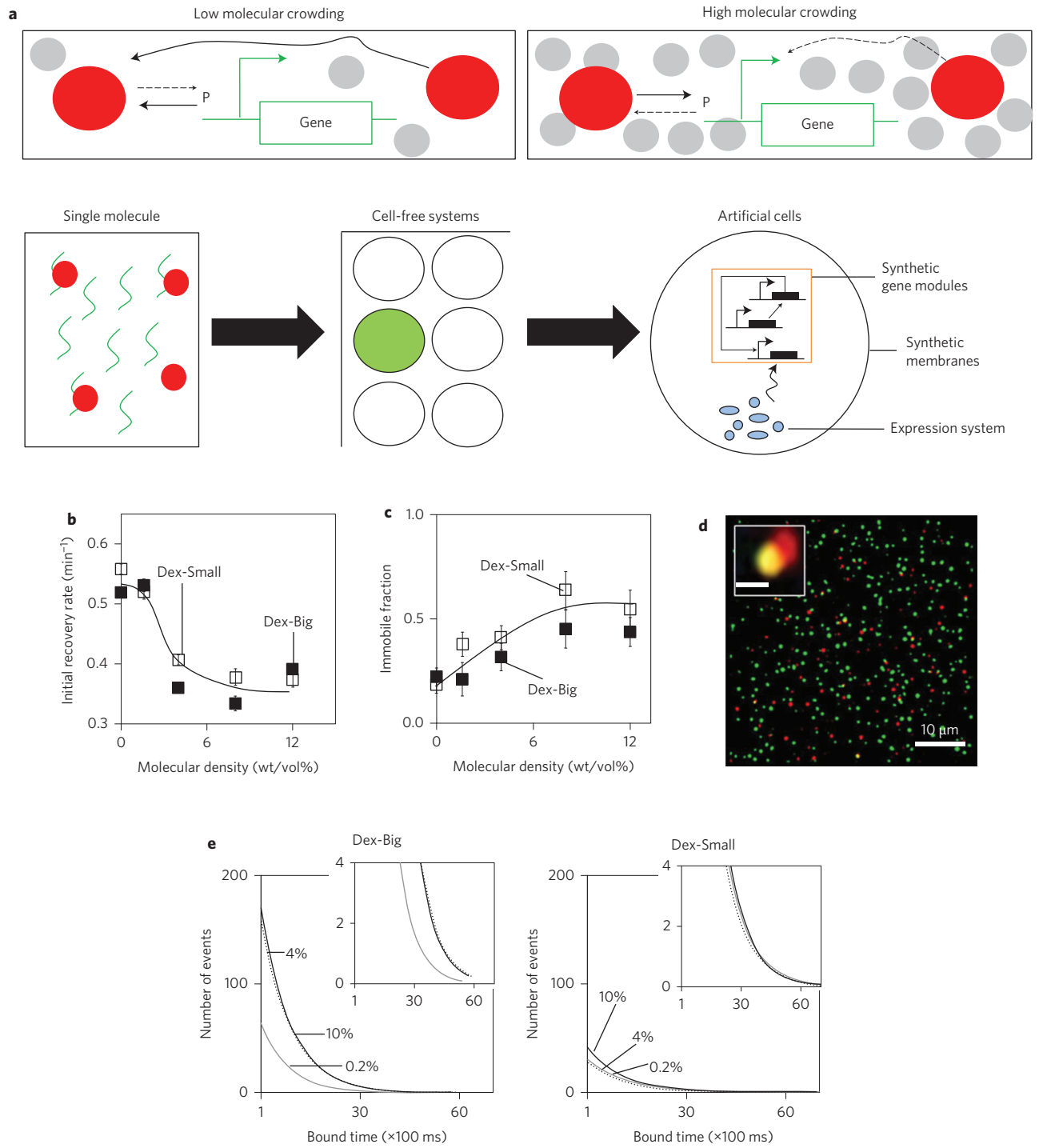

Figure 1 | Shaping gene expression in artificial cellular systems by molecular crowding. a, Macromolecular crowding, a key feature of natural cells, can dramatically influence biochemical kinetics (top panels). Molecular crowding (grey circles) can enhance binding between two molecules (red circles and promoter P), but decrease diffusion of molecules (top right panel). We studied the impact of molecular crowding on gene expression by bridging between microscopic single-molecule dynamics and macroscopic dynamics in both cell-free systems in 96-well plates and artificial cells. **b**, FRAP was conducted to study diffusion dynamics of RFP–T7 RNAP. Both big and small dextran molecules (Dex-Small = 6×10^3 g mol^{-1}, Dex-Big = 2×10^6 g mol^{-1}) significantly reduced the initial recovery rates of mobile T7 RNAP. Each error bar indicates one standard error of the mean (s.e.m.) of at least nine replicates. See Supplementary Fig. S3a and Supplementary section 'Fluorescent recovery after photo bleaching' for the detailed experimental setup. **c**, Both Dex-Small (open squares) and Dex-Big (filled squares) significantly increased the immobile fractions of RFP–T7 RNAP. Each error bar indicates one s.e.m. of at least nine replicates. Note that the differences in recovery dynamics were not due to then altered photostability of RFP, because crowding molecules did not affect the bleaching dynamics of RFP–T7 RNAP during the FRAP experiments (results not shown). **d**, RFP–T7 RNAP (red) co-localized with Cy3–P_{T7} (green) molecules. The image shows a typical frame of view with approximately 200 Cy3–P_{T7} molecules. Inset: single-molecule view of co-localized RFP–T7 RNAP and Cy3–P_{T7} molecules (scale bar, 533 nm). See Supplementary Fig. S4a and Supplementary section 'Setup of microscope for single molecule imaging' for detailed experimental setup. **e**, Dex-Big significantly increased the number of binding events and mean bound time as compared with Dex-Small. Each inset shows a zoomed-in view of the tail of the same distribution. Black lines represent 10% molecular density. Black dotted lines represent 4% molecular density. Grey lines represent 0.2% molecular density.

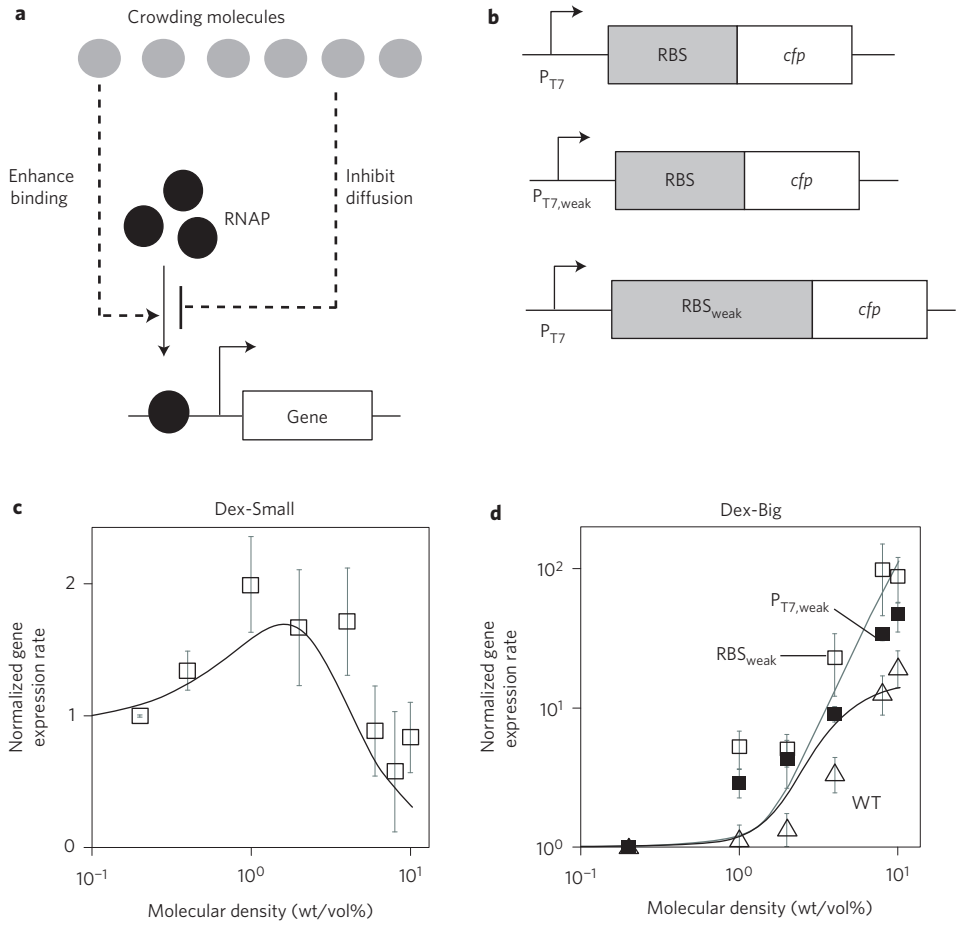

Figure 2 | Molecular crowding modulates dynamics of gene expression. a, A parsimonious model of gene expression in crowded environments. See equation (S1-10) for detailed mathematical models. **b**, Three genetic modules were constructed to study the impact of genetic elements on crowding effects. The first module is a base module that has wild-type genetic components. The second and third modules have either a weaker T7 promoter or a weaker RBS. **c**, Gene expression rates in environments containing small crowding molecules. Both modelling (black line) and experimental (open black squares) results show that gene expression rates exhibit a biphasic response with increasing densities of Dex-Small. A paired *t*-test shows that gene expression rates at 1% density are significantly higher than gene expression rates at both 0.2% density ($P = 0.02$) and 10% density ($P = 0.0008$). Each error bar indicates one s.e.m. of at least four replicates. Each gene expression rate was normalized by the basal rate with 0.2% crowding molecules. **d**, Gene expression rates in environments containing big crowding molecules. Our model predicts that a big crowding molecule will increase gene expression rates (black line) and that a weaker genetic component (Fig. 2b) will result in a higher fold increase in gene expression rates (grey line). Consistent with the predictions, gene expression rates increased with increasing densities of Dex-Big (open triangles). With either a weak T7 promoter ($pT7_{weak}$, filled black squares) or a weak RBS (RBS_{weak}, open black squares), gene expression rates increased more significantly than with the wild-type module (WT, open triangles). A paired *t*-test shows that for each molecular density (≥1%), normalized gene expression rates of both $pT7_{weak}$ and RBS_{weak} modules are significantly higher than normalized gene expression rates of the wild-type module ($P < 0.04$). Each error bar indicates one s.e.m. of at least five replicates.

RNAP (Fig. 1c). Based on existing diffusion models[29], these increased immobile fractions are probably a result of greater subdiffusion fractions of RFP–T7 RNAP in the crowded environments, in which the polymerase explores a smaller space than predicted by classical Brownian dynamics. Therefore, our findings suggest that both Dex-Small and Dex-Big reduce the diffusion of RFP–T7 RNAP.

Impact on binding of T7RNAP to a T7 promoter

In addition to the diffusion of macromolecules, gene transcription is sensitive to binding between transcription factors and promoters[30,31]; this is essential to understanding the impact of molecular crowding on gene expression. To measure the binding between RFP–T7 RNAP and a P_{T7} promoter, we built on our FRAP experiments and conjugated biotinylated Cy3–P_{T7} DNA molecules onto PEG surfaces via avidin–biotin linkages (Supplementary Fig. S4). When Cy3–P_{T7} was immobilized on the surface, RFP–T7 RNAP would freely diffuse in the chamber and bind to P_{T7} on the surface. We used this approach[30] to measure co-localization of RFP–T7 RNAP with Cy3–P_{T7}, which would suggest that there was binding between them (Fig. 1d; Supplementary Fig. S5a, Movie S2). We expected that a lower dissociation rate constant would shift the mean of the bound time distribution to a higher bound time, and a higher association rate constant would increase the number of detected binding events at low bound times. With Cy3–P_{T7}, 10% Dex-Big significantly increased the number of binding events by ~100% compared with the control (0.2% Dex-Big) (Fig. 1e), suggesting an increased association rate constant. With 10% Dex-Big, the mean of the bound time distribution also increased by ~100 ms compared with the control (0.2% Dex-Big), suggesting a decreased dissociation rate constant. In contrast, 10% Dex-Small only increased the number of binding events by ~25% compared with the control (0.2% Dex-Small). These observations suggest that Dex-Big lowered the dissociation rate constants and increased the association rate constants between T7 RNAP and P_{T7} more significantly than Dex-Small, which is consistent with a

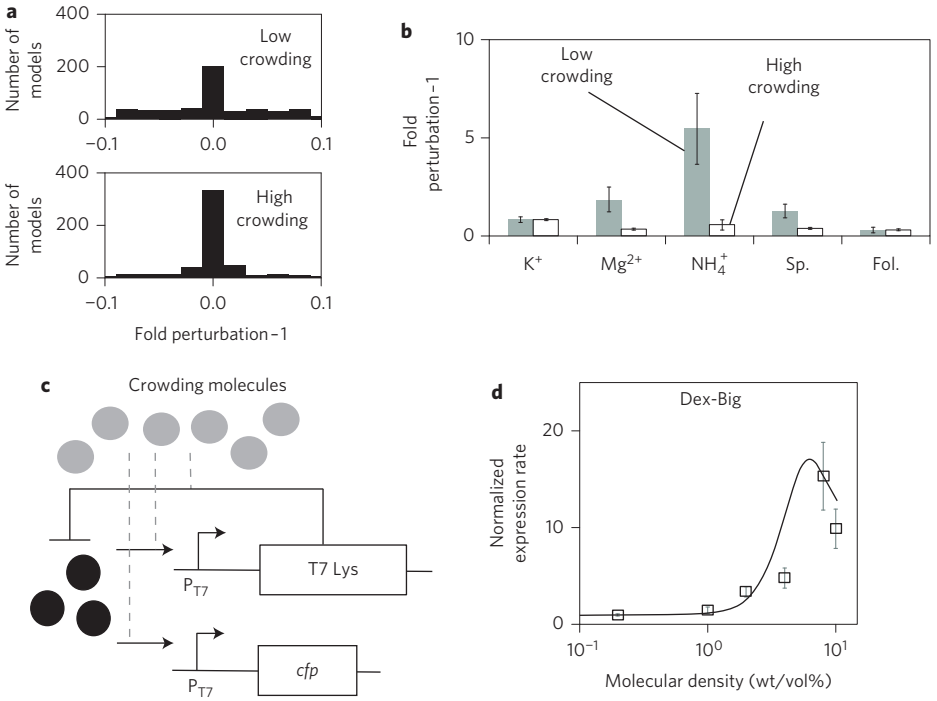

Figure 3 | Molecular crowding increases robustness of gene expression. a, Modelling prediction of gene expression robustness. A highly crowded environment results in a narrow distribution of fold gene-expression perturbation (bottom panel), suggesting that molecular crowding decreases the fluctuation of gene expression rates due to the perturbation of gene environmental factors. In contrast, a low crowding environment results in significant perturbation of the system (top panel). See Supplementary section 'Mathematical modeling' and Supplementary equation (S11) for detailed model description. **b**, Absolute fold perturbation of gene expression rates using five chemicals. The system was perturbed by changing the concentrations of potassium glutamate (K^+), magnesium acetate (Mg^{2+}), ammonium acetate (NH_4^+), spermidine (Sp.) and folinic (Fol.) acids. Consistent with our model predictions, gene expression rates were less perturbed in a highly crowded environment than in a low crowded environment. Grey bars represent low crowding environments without Dex-Big. Black open bars represent high crowding environments with 10% Dex-Big. Each error bar indicates one s.e.m. of four replicates. **c**, Schematic of interactions between molecular crowding and a negative feedback loop. A negative feedback loop was constructed using a T7 lysozyme that binds to T7 RNAP and inhibits transcription from the P_{T7} promoter. Molecular crowding could impact both the binding of T7 RNAP to the promoter and the binding between T7 RNAP and T7 Lys (grey dotted lines). **d**, Gene expression rates of a negative feedback loop with increasing crowding densities. Both modelling (black line) and experimental (open squares) results show that the negative feedback circuit generated a biphasic response of gene expression rates that peaked at 8% Dex-Big (open squares). A *t*-test shows that gene expression rates at 8% density are significantly higher than gene expression rates at both 0.2% density ($P = 0.003$) and 10% density ($P = 0.001$). Each error bar represents the s.e.m. of seven replicates. Each gene expression rate was normalized by the basal rate with 0.2% crowding molecules.

general theory of molecular crowding that suggests a larger enhancement of molecular binding by large crowding molecules than by small crowding molecules[20]. Using a control DNA without the P_{T7} promoter, co-localization of RFP–T7 RNAP with Cy3 was negligible (Supplementary Fig. S5b), suggesting that the observation was not due to non-specific interactions between T7 RNAP and either the PEG surface or DNA.

Molecular crowding impacts gene expression dynamics

To gain insight into connections between the microscopic dynamics observed using single-molecule imaging and gene expression dynamics, we created a parsimonious model based on previous models of molecular crowding[17] and qualitative results obtained from the FRAP and single-molecule experiments (see Fig. 2a, Supplementary Fig. S6). Based on the model, we first predicted the expression dynamics of a genetic module with a native P_{T7} promoter that regulates the expression of CFP as a reporter of gene expression (Fig. 2b). Our model predicts that a small crowding molecule would result in a biphasic response, with gene expression rates first rising with increasing crowding densities, but then decreasing after reaching a specific crowding density (Fig. 2c, black line). The biphasic response arises because Dex-Small only increases the number of binding events by ~25% (Fig. 1e), but significantly reduces the diffusion of T7 RNAP (Fig. 1b,c). The predicted biphasic dynamic response was indeed observed with our cell-free expression system, which consisted of an S12 bacterial extract, an S12 supplement and Dex-Small (Fig. 2c, black squares; see Supplementary section 'S12 bacterial extract preparation'). The cell-free expression system is a synthetic system that couples transcription and translation and has been used to create artificial cells[13]. In contrast, both our model and experiments show that Dex-Big causes a monotonic increase in gene expression rates with increasing crowding densities (Fig. 2d, Supplementary Fig. S7), because Dex-Big significantly increases the association rate constant and reduces the dissociation rate constant between T7 RNAP and P_{T7} promoter (Fig. 1e). Additional tests using alternative crowding agents, including Ficoll 400 (400×10^3 g mol^{-1}), PEG-100k (100×10^3 g mol^{-1}) and PEG8000 (8×10^3 g mol^{-1}), suggest that the size-dependent impact of molecule crowding on gene expression rates is probably a generic phenomenon (Supplementary Fig. S8a). Specifically, Ficoll-400 is approximately the same size as Dex-Big and resulted in monotonically increasing expression rates. PEG-8000, a small crowding molecule, caused biphasic expression rates, and PEG-100k, a crowding molecule of intermediate size, significantly increased gene expression rates compared with PEG8000. Similar to the observed impact of molecular crowding on the dynamics of nuclear proteins in heterochromatin[32], our results suggest that the

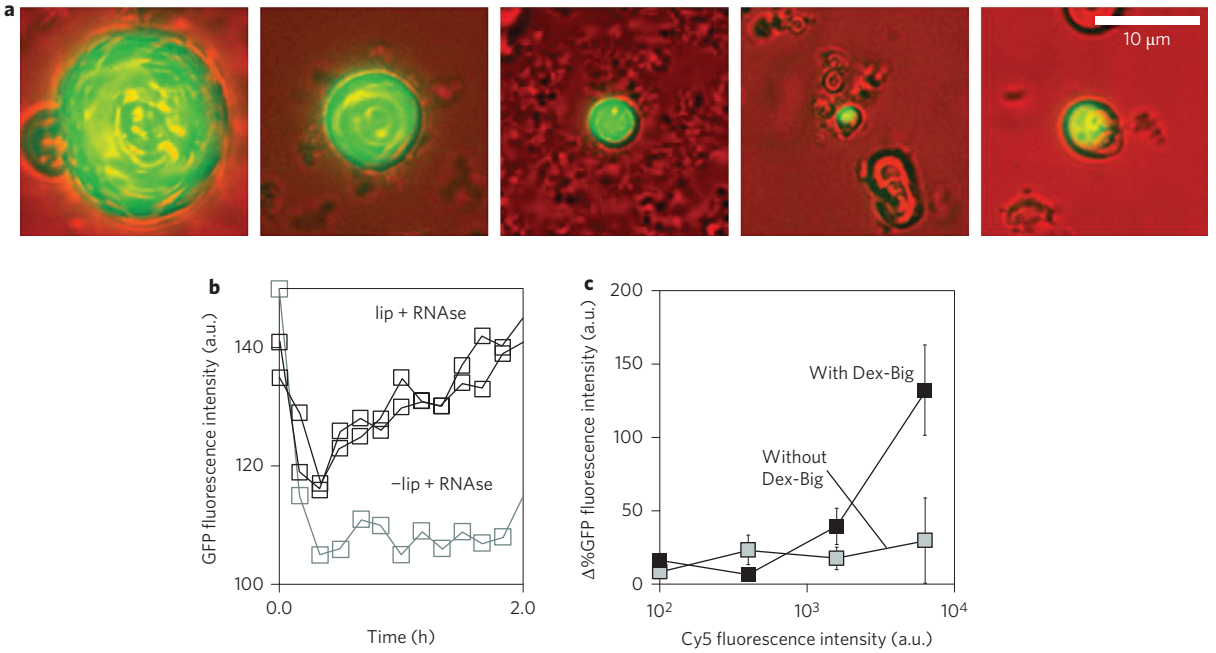

Figure 4 | Volume-dependent impact of molecular crowding in artificial cells. a, Fluorescence images of artificial cells. The artificial cells encapsulate a synthetic genetic construct that expresses GFP within lipid bilayers. See Supplementary section 'Preparation of liposomes' for the experimental protocol. The scale bar in the last panel applies to all panels. **b**, Temporal dynamics of GFP expression. With liposomes (black squares), the fluorescence intensity of GFP increased after the 30th minute. In contrast, without liposomes (grey squares), the fluorescence intensity of GFP remained constant. RNAse A inhibited gene expression outside artificial cells by degrading RNAs. RNAse A was added in the medium to ensure that the observed GFP expression inside the artificial cells was not due to either transport of GFP from the outside of artificial cells or attachment of GFP on the surfaces of artificial cells. **c**, GFP expression inside artificial cells with and without Dex-Big crowding molecules. Molecular crowding enhances gene expression in large artificial cells (fluorescence intensity of Cy5 > 2,000 a.u.). Each Δ%GFP intensity was calculated by using the percentage differences between mean GFP fluorescence intensity of artificial cells with and without pT7-GFP plasmids (see Supplementary section 'Preparation of artificial cells'). Each error bar represents one s.e.m. of five replicates.

molecular composition of genetic microenvironments can distinctly modulate gene expression rates.

To respond to changing environments, natural cells could couple crowding densities with both promoters and ribosomal binding sites (RBSs) to modulate gene expression rates[33]. To investigate this link between genetic components and molecular crowding, we constructed two additional genetic modules, with either a weak P_{T7} promoter ($P_{T7,weak}$) or a weak RBS (RBS_{weak}) (Fig. 2b), which resulted in lower gene expression rates (Supplementary Fig. S8b). Previous studies have also demonstrated that these genetic components exhibit higher dissociation rate constants[34,35] between T7 RNAP and $P_{T7,}$ and ribosome and RBS, when compared with the components used in the original module (Fig. 2b). Based on kinetic information, mathematical modelling predicts that these modules would result in higher fold changes in gene expression rates with increasing crowding densities when compared with the base module (Fig. 2d), as a result of a faster decrease in the dissociation constants of macromolecules and their respective binding sites with increasing crowding densities. Consistent with our model predictions, the gene expression rates of both $P_{T7,weak}$ and RBS_{weak} increase more than those of the base module with increasing crowding densities (Fig. 2d).

Increased robustness of gene expression

Molecular crowding is a cellular feature that has been maintained throughout evolution[36], suggesting that molecular crowding could be essential in maintaining the robustness of system dynamics, which is a hallmark of biological systems. To allow for a more systematic assessment of this hypothesis than would be possible experimentally, we first created two parameter sets using the same mathematical model, each representing either a low or a high crowding environment. We next used computer simulations to emulate perturbations of these base models by randomizing their kinetic constants within ten times their base values (see Supplementary section 'Robustness tests'). The changes in the gene expression rates of perturbed models, compared with the base models, are quantified as 'fold perturbations' to estimate the robustness of the systems (Fig. 3a), where a high absolute value indicates a significant perturbation to a system. The fold perturbations are approximately zero in highly crowded conditions. In contrast, in a low crowding environment, fold perturbations are non-zero, showing that the system is more sensitive to the parameter perturbations. These simulation results suggest that molecular crowding may support the robustness of gene expression in natural cells. Furthermore, these results are consistent with the simulation results of a stochastic model that includes intrinsic noise (see Supplementary section 'Stochastic model' Supplementary Fig. S9a).

We experimentally tested the impact of molecular crowding on system robustness by changing the concentrations of potassium, magnesium, ammonium, spermidine and folinic acid (Fig. 3b) in cell-free expression systems. These chemicals modulate both the stability and binding of macromolecules[37]. Our experimental results show that a low crowding environment (0.2% Dex-Big) results in higher perturbations of gene expression than a highly crowded environment (10% Dex-Big) for magnesium, ammonium and spermidine. Furthermore, we tested if the robustness of gene expression could be fine-tuned using intermediate crowding densities. We observed that ammonium indeed caused a monotonic decrease in fold perturbations with increasing crowding densities (Supplementary Fig. S9b).

Modulation with a negative feedback loop

In addition to genetic elements, gene circuit dynamics are known to be modulated by negative feedback loops, which are the most

ubiquitous motif in natural gene circuits[38], probably due to their noise reduction and autoregulatory roles. Here, we tested if molecular crowding can modulate gene expression of a negative feedback loop. To gain insight into interactions between feedback loops and molecular crowding, we simulated the expression dynamics of a negative feedback loop consisting of a T7 lysozyme that binds to T7 RNA polymerase and inhibits T7 RNAP transcription activities (Fig. 3c). We assume that binding between T7 RNAP and P_{T7} would be enhanced at a smaller crowding density relative to the binding between T7 RNAP and T7 lysozyme, which is based on existing theories of molecular crowding[20]. As a result, our model predicts that the negative feedback loop would cause biphasic expression rates in environments with large crowding molecules (Fig. 3d, black line). Our experimental results support the model prediction, as expression rates are maximized at 8% crowding density (Fig. 3d, black squares). We note that this is not due to the increased metabolic burden in the expression systems (Supplementary Fig. S10a). To further corroborate our model, we investigated the impact of a lower T7 RNAP concentration on gene expression rates. Based on our model, we expected similar biphasic gene expression rates with a negligible shift in the crowding density that maximizes gene expression rates (Supplementary Fig. S10b, black line). To test the prediction, we modulated the amount of T7 RNAP by controlling the ratio of cell-free expression systems that either contain T7 RNAP or do not contain T7 RNAP, resulting in a 75% reduction in gene expression rates. Based on this system, we observed the same biphasic gene expression rates with a maximum rate at 8% crowding density (Supplementary Fig. S10b, black squares).

Modulation by reaction volumes

In natural cells, compartmentalization is the hallmark for creating unique functional units, such as Golgi, nuclei and mitochondria. Based on our results with cell-free systems, we hypothesized that crowding could similarly affect gene expression in physiologically relevant volumes. To test this hypothesis, we constructed artificial cells that consisted of phospholipid membranes, synthetic expression systems and a genetic construct (Fig. 4a; Supplementary Fig. S11). We created artificial cells (radii ranging from 100 nm to 10 μm) that expressed green fluorescent proteins (GFP), using a genetic construct. To ensure that the GFP was expressed inside the artificial cells, we added RNAse to inhibit RNA synthesis outside the artificial cells (Fig. 4b; Supplementary Fig. S12a). Without liposomes, RNAse inhibited GFP expression (Fig. 4b), but with liposomes to protect the enclosed volumes, RNAse did not inhibit GFP expression. We next investigated the influence of cell volume on the impact of molecular crowding. Specifically, we used the integrated intensity of a Cy5 fluorescent dye inside artificial cells as a surrogate of encapsulation volume (Supplementary Fig. S12b–d)[39]. Based on our results using cell-free expression systems that essentially resulted in semi-infinite reaction volumes, we expected that molecular crowding would exert a larger impact on gene expression in large volumes than in small volumes. Indeed, we observed that Dex-Big increased GFP expression in artificial cells of large volumes compared with that in artificial cells without Dex-Big (Fig. 4c, fluorescence intensity of Cy5 $>$ 2,000 a.u.; Supplementary Fig. S12e). This is probably due to the reduced reaction rates in large volumes without molecular crowding. As the size of the artificial cells decreased, GFP levels in artificial cells with Dex-Big approached the GFP levels of artificial cells without Dex-Big. These findings indicate that in our synthetic cellular systems, compartmentalization and crowding can play essential roles in controlling gene expression, factors that need to be considered in both mimicking genetic systems for applications in synthetic biology and accurately modelling cellular biochemistry for systems biology.

Discussion

In this study, we have demonstrated that molecular crowding increases the robustness of gene expression and that molecular crowding can be harnessed for the control of a basic genetic construct in artificial cells. We have also shown the impact of molecular crowding on the dynamics of T7 RNAP and how the influence of molecular crowding on gene expression rates can be modulated using genetic components, a negative feedback loop and the size of the crowding molecules. Our results suggest that the construction of both *in vitro* circuits[4] and programmable artificial cells[13] would have to take into account molecular crowding effects, which would be important in modulating system dynamics. Our findings underscore how scientists could harness molecular crowding for developing advantages in engineered cell functions such as gene expression, metabolic pathways and cellular computing. For natural systems[36], our conclusions with respect to the impact of molecular crowding sizes, strength of genetic components and network architectures could potentially explain how gene circuit dynamics are modulated by changing environments. Our studies would also impact *in vitro* studies of gene expression and their extension to *in vivo* environments that are crowded with molecules. As we move towards a bottom up and *a priori* approach of constructing either artificial cells or cells with completely designed genomes, it is critical to understand the impact of crowded environments on system robustness and then exploit these design principles to our advantage, just as natural cells have already accomplished. Furthermore, systems biology has begun to take advantage of synthetic cellular systems as high-throughput methods to characterize interactions between cellular components[40]. In this context, it is critical to understand how molecular crowding can fundamentally impact interactions between cellular components and generate emergent dynamics that cannot be predicted or controlled without considering molecular crowding.

Received 20 January 2013; accepted 10 June 2013;
published online 14 July 2013

References

1. Gibson, D. G. *et al.* Complete chemical synthesis, assembly, and cloning of a *Mycoplasma genitalium* genome. *Science* **319,** 1215–1220 (2008).
2. Pinheiro, V. B. *et al.* Synthetic genetic polymers capable of heredity and evolution. *Science* **336,** 341–344 (2012).
3. Nawroth, J. C. *et al.* A tissue-engineered jellyfish with biomimetic propulsion. *Nature Biotechnol.* **30,** 792–797 (2012).
4. Kim, J. & Winfree, E. Synthetic *in vitro* transcriptional oscillators. *Mol. Syst. Biol.* **7,** 465 (2011).
5. Fernandes, R., Roy, V., Wu, H. C. & Bentley, W. E. Engineered biological nanofactories trigger quorum sensing response in targeted bacteria. *Nature Nanotech.* **5,** 213–217 (2010).
6. Murtas, G., Kuruma, Y., Bianchini, P., Diaspro, A. & Luisi, P. L. Protein synthesis in liposomes with a minimal set of enzymes. *Biochem. Biophys. Res. Commun.* **363,** 12–17 (2007).
7. Schroeder, A. *et al.* Remotely activated protein-producing nanoparticles. *Nano Lett.* **12,** 2685–2689 (2012).
8. Martino, C. *et al.* Protein expression, aggregation, and triggered release from polymersomes as artificial cell-like structures. *Angew. Chem. Int. Ed.* **51,** 6416–6420 (2012).
9. Ishikawa, K., Sato, K., Shima, Y., Urabe, I. & Yomo, T. Expression of a cascading genetic network within liposomes. *FEBS Lett.* **576,** 387–390 (2004).
10. Leduc, P. R. *et al.* Towards an *in vivo* biologically inspired nanofactory. *Nature Nanotech.* **2,** 3–7 (2007).
11. Gardner, P. M., Winzer, K. & Davis, B. G. Sugar synthesis in a protocellular model leads to a cell signalling response in bacteria. *Nature Chem.* **1,** 377–383 (2009).
12. Mansy, S. S. *et al.* Template-directed synthesis of a genetic polymer in a model protocell. *Nature* **454,** 122–125 (2008).
13. Noireaux, V., Maeda, Y. T. & Libchaber, A. Development of an artificial cell, from self-organization to computation and self-reproduction. *Proc. Natl Acad. Sci. USA* **108,** 3473–3480 (2011).
14. Chang, T. M. Therapeutic applications of polymeric artificial cells. *Nature Rev. Drug Discov.* **4,** 221–235 (2005).

15. Jewett, M. C., Calhoun, K. A., Voloshin, A., Wuu, J. J. & Swartz, J. R. An integrated cell-free metabolic platform for protein production and synthetic biology. *Mol. Syst. Biol.* **4,** 220 (2008).
16. Ellis, R. J. Macromolecular crowding: obvious but underappreciated. *Trends Biochem. Sci.* **26,** 597–604 (2001).
17. Morelli, M. J., Allen, R. J. & Wolde, P. R. Effects of macromolecular crowding on genetic networks. *Biophys. J.* **101,** 2882–2891 (2011).
18. Zimmerman, S. B. & Trach, S. O. Estimation of macromolecule concentrations and excluded volume effects for the cytoplasm of *Escherichia coli*. *J. Mol. Biol.* **222,** 599–620 (1991).
19. Minton, A. P. The influence of macromolecular crowding and macromolecular confinement on biochemical reactions in physiological media. *J. Biol. Chem.* **276,** 10577–10580 (2001).
20. Minton, A. P. The effect of volume occupancy upon the thermodynamic activity of proteins – some biochemical consequences. *Mol. Cell. Biochem.* **55,** 119–140 (1983).
21. Li, G-W., Berg, O. G. & Elf, J. Effects of macromolecular crowding and DNA looping on gene regulation kinetics. *Nature Phys.* **5,** 294–297 (2009).
22. Beg, Q. K. *et al.* Intracellular crowding defines the mode and sequence of substrate uptake by *Escherichia coli* and constrains its metabolic activity. *Proc. Natl Acad. Sci. USA* **104,** 12663–12668 (2007).
23. Richter, K., Nessling, M. & Lichter, P. Experimental evidence for the influence of molecular crowding on nuclear architecture. *J. Cell Sci.* **120,** 1673–1680 (2007).
24. Elcock, A. H. Models of macromolecular crowding effects and the need for quantitative comparisons with experiment. *Curr. Opin. Struct. Biol.* **20,** 196–206 (2010).
25. Schoen, I., Krammer, H. & Braun, D. Hybridization kinetics is different inside cells. *Proc. Natl Acad. Sci. USA* **106,** 21649–21654 (2009).
26. Phillip, Y., Sherman, E., Haran, G. & Schreiber, G. Common crowding agents have only a small effect on protein–protein interactions. *Biophys. J.* **97,** 875–885 (2009).
27. Mika, J. T. & Poolman, B. Macromolecule diffusion and confinement in prokaryotic cells. *Curr. Opin. Biotechnol.* **22,** 117–126 (2011).
28. Laurent, T. C. The interaction between polysaccharides and other macromolecules. 5. The solubility of proteins in the presence of dextran. *Biochem. J.* **89,** 253–257 (1963).
29. Feder, T. J., Brust-Mascher, I., Slattery, J. P., Baird, B. & Webb, W. W. Constrained diffusion or immobile fraction on cell surfaces: a new interpretation. *Biophys. J.* **70,** 2767–2773 (1996).
30. Friedman, L. J. & Gelles, J. Mechanism of transcription initiation at an activator-dependent promoter defined by single-molecule observation. *Cell* **148,** 679–689 (2012).
31. Wang, Y., Guo, L., Golding, I., Cox, E. C. & Ong, N. P. Quantitative transcription factor binding kinetics at the single-molecule level. *Biophys. J.* **96,** 609–620 (2009).
32. Bancaud, A. *et al.* Molecular crowding affects diffusion and binding of nuclear proteins in heterochromatin and reveals the fractal organization of chromatin. *EMBO J.* **28,** 3785–3798 (2009).
33. Burg, M. B., Kwon, E. D. & Kultz, D. Osmotic regulation of gene expression. *FASEB J.* **10,** 1598–1606 (1996).
34. Martin, C. T. & Coleman, J. E. Kinetic analysis of T7 RNA polymerase–promoter interactions with small synthetic promoters. *Biochemistry* **26,** 2690–2696 (1987).
35. Gardner, T. S., Cantor, C. R. & Collins, J. J. Construction of a genetic toggle switch in *Escherichia coli*. *Nature* **403,** 339–342 (2000).
36. Spitzer, J. & Poolman, B. The role of biomacromolecular crowding, ionic strength, and physicochemical gradients in the complexities of life's emergence. *Microbiol. Mol. Biol. Rev.* **73,** 371–388 (2009).
37. Chen, H. Z. & Zubay, G. Prokaryotic coupled transcription-translation. *Methods Enzymol.* **101,** 674–690 (1983).
38. Milo, R. *et al.* Network motifs: simple building blocks of complex networks. *Science* **298,** 824–827 (2002).
39. Sunami, T. *et al.* Femtoliter compartment in liposomes for *in vitro* selection of proteins. *Anal. Biochem.* **357,** 128–136 (2006).
40. Harris, D. C. & Jewett, M. C. Cell-free biology: exploiting the interface between synthetic biology and synthetic chemistry. *Curr. Opin. Biotechnol.* **23,** 672–678 (2012).

Acknowledgements

The authors thank members of the LeDuc and Schwartz laboratories, the group of the Center for Mechanical Technology and Automation at University of Aveiro in Portugal, Dr. Shuqiang Huang, Dr. Gang Bao, and Dr. Lingchong You for discussions and comments, and R. Murphy, A. Mitchell, B. Armitage, T. Lee, F. Lanni and the Molecular Biosensor and Imaging Center for providing access to equipment. This work was partially supported by a Lane Postdoctoral Fellowship (C.T.), a Society in Science – Branco Weiss Fellowship (C.T.), NIH 1R01GM086237 (M.B. & S.S.), NIH 8U54GM103529 (M.B. & S.S.), NIH 1R01AI076318 (R.S), NIH 1R01CA140214 (R.S), NSF CMMI-1100430 (P.L.), NSF CMMI-0856187 (P.L.), NSF CMMI-1160840 (P.L.), ONR N000140910215 (P.L.), and NSF CPS-1135850 (P.L.).

Author contributions

C.T., S.S., R.S. and P.L. conceived the research and designed the experiments. C.T. and S.S. performed the experiments. C.T. carried out the modelling analysis. C.T., S.S., M.B. and P.L. provided materials and reagents. C.T., R.S. and P.L. interpreted the results and wrote the manuscript, with critical input from S.S. and M.B. All authors approved the manuscript.

Additional information

Supplementary information is available in the online version of the paper. Reprints and permissions information is available online at www.nature.com/reprints. Correspondence and requests for materials should be addressed to R.S. and P.L.

Competing financial interests

The authors declare no competing financial interests.